

Structural and dielectric properties of $\text{Pb}_{(1-x)}(\text{Na}_{0.5}\text{Sm}_{0.5})_x\text{TiO}_3$ ceramics

Arun Kumar Yadav¹, Anita¹, Sunil Kumar¹, V. Raghavendra Reddy³, Parasharam M. Shirage^{1,2}, Sajal Biring⁴, Somaditya Sen^{1,2*}

¹Discipline of Metallurgy Engineering and Materials Science, Indian Institute of Technology, Khandwa Road, Indore-453552 India

²Discipline of Physics, Indian Institute of Technology, Khandwa Road, Indore-453552 India

³UGC-DAE Consortium for Scientific Research, University Campus, Khandwa Road, Indore-452001, India

⁴Electronic Engg., Ming Chi University of Technology, New Tapei City, Taiwan

Corresponding Author: sens@iiti.ac.in

Abstract:

A correlation between structure and vibrational properties related to a ferroelectric to paraelectric phase transition in perovskite $\text{Pb}_{(1-x)}(\text{Na}_{0.5}\text{Sm}_{0.5})_x\text{TiO}_3$ ($0 \leq x \leq 0.5$) (PNST- x) polycrystalline powders is discussed. Substitution leads to reduction of tetragonality which is associated with a shift of the phase transition to lower temperatures. The nature of the phase transition gets diffused with increasing substitution.

Keywords: Structural properties, Raman spectroscopy, Dielectric, Phase transition.

Introduction

PbTiO_3 is known to be a strong ferroelectric perovskite compound. A structural phase transition from tetragonal ($P4mm$) to cubic ($Pm3m$) phase at 763K is observed in PbTiO_3 . Tetragonality, measured by c/a ratio is frequently related to ferroelectric properties. For PbTiO_3 , c/a ratio is ~ 1.06 at room temperature [1-5]. Properly substituted PbTiO_3 has different applications as capacitors, nonvolatile memories, ultrasonic transducers, pyroelectric infrared sensors, piezoelectric actuators due to their highly anisotropic nature of elastic, piezoelectric, and electro-optic properties etc. [6-8].

Physical properties and device applications of ferroelectric perovskite (ABO_3) compounds like PbTiO_3 and BaTiO_3 have been studied extensively due to their technological importance. Based on the fact that PbTiO_3 is toxic and volatile in nature and not environmental friendly many reduced lead content ferroelectric materials has been investigated, such as $\text{Pb}(\text{Mg}_{1/3}\text{Nb}_{2/3})\text{O}_3\text{-PbTiO}_3$, $\text{Ba}(\text{Mg}_{1/3}\text{Nb}_{2/3})\text{O}_3\text{-}x\text{PbTiO}_3$, $\text{Ba}(\text{Zn}_{1/3}\text{Nb}_{2/3})\text{O}_3\text{-}x\text{PbTiO}_3$, $\text{Ba}(\text{Yb}_{1/2}\text{Nb}_{1/2})\text{O}_3\text{-}x\text{PbTiO}_3$, $\text{Ba}(\text{Sc}_{1/2}\text{Nb}_{1/2})\text{O}_3\text{-}x\text{PbTiO}_3$ and $\text{BaSnO}_3\text{-}x\text{PbTiO}_3$ [9-12]. Isovalent or heterovalent substitution on Pb^{2+} site, lattice anisotropy is reduced.

Diffuse phase transition in dielectric response has a broad peak with temperature rather than sharp peak in normal ferroelectric. The diffusion of the peak comes from the fact that the

phase transition in different micro regions takes place at different temperatures. The signature of this is typically due to heterovalent disorder substitution [13-14].

Motivation of our research is to explore the effect of substitution of *Pb* by *Na/Sm* on the structural, vibrational and dielectric properties of the newly synthesized compounds of $\text{Pb}_{(1-x)}(\text{Na}_{0.5}\text{Sm}_{0.5})_x\text{TiO}_3$ with ($0 \leq x \leq 0.5$). Although PbTiO_3 is an extensively studied material, however, hardly any report is available in the literature on $\text{Pb}_{(1-x)}(\text{Na}_{0.5}\text{Sm}_{0.5})_x\text{TiO}_3$ compounds.

Synthesis

Polycrystalline powders of $\text{Pb}_{(1-x)}(\text{Na}_{0.5}\text{Sm}_{0.5})_x\text{TiO}_3$ ($0 \leq x \leq 0.5$) ceramics were prepared using sol-gel process. Precursors were used to synthesize these materials, Lead (II) nitrate (99.999%, Alfa Aesar), Samarium oxide (99.999%, Alfa Aesar), Sodium Nitrate and Dihydroxybis (ammonium lactate) titanium (IV), 50% w/w aqua solution (Alfa Aesar). The stoichiometric solutions of each precursor were prepared with double distilled water in a separate beaker. Samarium oxide is soluble in dilute nitric acid and it was added to the titanium solution followed by the addition of the sodium and lead solution. A solution of citric acid and ethylene glycol of 1:1 molar ratio was prepared in a separate beaker as gel former and was thereafter added after vigorous stirring and heating ($\sim 70^\circ\text{C}$) on hot plate. After mixing of all precursors in a beaker we added ammonium hydroxide to maintain the pH value of the solution at 8. The solution was continuously stirred and heated ($\sim 70^\circ\text{C}$) on the hot plate to form gel. After that, gels were burnt into a big beaker of two liter inside a fume hood. Burnt powders were heated at 450°C for 12 h as a denitrification of the powder. Carefully grinding of these powders were mixed with 5% PVA solution as a binder and uniaxially pressed into discs of 13 mm diameter and 1.5 mm thickness. These pellets were sintered at 600°C for 6 h to burn out the binder continued with 1050°C for 4h.

X-ray powder diffraction was performed using a Bruker D2 Phaser X-ray Diffractometer to ensure the phase purity of the sintered samples. The HR Raman spectrometer was done with Czerny-Turner type achromatic spectrograph with spectral resolution of $0.4\text{ cm}^{-1}/\text{pixel}$ and the source of excitation is 632.8 nm. Microstructure and grain size of the sintered pellets were investigated by Supra55 Zeiss field emission scanning electron microscope.

For electrical property measurements, sintered pellets with relative density around 90-92% of the theoretical value were prepared. Electrodes were prepared using silver paste painted on both side of the sintered pellet. The silver coated pellets were cured at 550°C for 10 minutes. To avoid any moisture to get adhered to the sample, we heated the samples at 200°C for 10 minutes. Dielectric response was measured using a Newtons 4th LTD PSM 1735 phase sensitive with a signal strength of 0.5 V. Ferroelectric (*P-E*) studies were carried out by ferroelectric loop (*P-E*) tracer (M/s Radiant Instruments, USA). During the ferroelectric measurements, the samples were immersed in silicone oil to prevent electric arcing, at high applied voltages.

Results and discussion

X-ray powder diffraction (XRD) patterns of the PNST- x powders with $0 \leq x \leq 0.5$, were analyzed (Fig. 1). A tetragonal $P4mm$ phase is detected for compositions $x = 0, 0.10, 0.20, 0.30$ and 0.40 and cubic $Pm3m$ phase for $x=0.5$. There are two extra peaks of trace amount of Sm_2TiO_5 at 27.6° and 29.3° . This Sm_2TiO_5 phase may be due to volatile nature of Pb . A LeBail profile fitting of the XRD data was done with Topas3.2 software to calculate lattice parameters. With increasing substitution, the separation between the (001) and (100) peaks reduces and thereafter merges at $x=0.5$. That Na/Sm is substituting lead is indicated from the continuous decrease in the volume of the substituted compounds, due to decrease of lattice parameter ‘ c ’, while ‘ a ’ is nearly constant. The average ionic radii of A-site are calculated using the relation [15]:

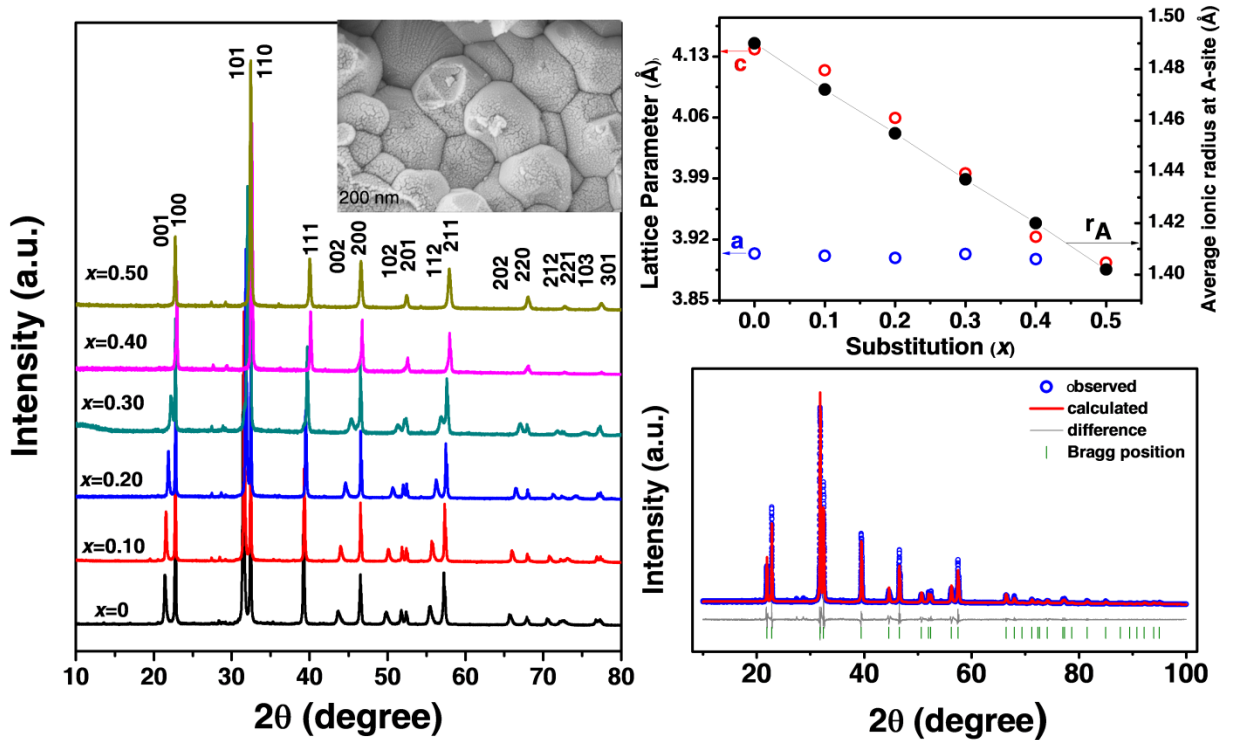


Fig. 1. (a) X-ray diffraction patterns of the compound $\text{Pb}_{(1-x)}(\text{Na}_{0.5}\text{Sm}_{0.5})_x\text{TiO}_3$ ($0 \leq x \leq 0.5$) (b) Lattice parameter and average ionic radius at A-site versus substitutions x (c) LeBail profile fitting for $x=0.20$ with tetragonal space group $P4mm$.

$$r_A = [(1-x)r_{\text{Pb}^{2+}}] + \left[\frac{x}{2}(r_{\text{Sm}^{3+}} + r_{\text{Na}^{+}})\right] \quad (1)$$

where, Shannon's radii values are given as, $r_{\text{Pb}^{2+}} = 1.49 \text{ \AA}$, $r_{\text{Sm}^{3+}} = 1.24 \text{ \AA}$, and $r_{\text{Na}^{+}} = 1.39 \text{ \AA}$. Note that r_A decreases linearly with substitution [Table 1]; r_A also determines the composition dependence of the tolerance factor (t), calculated by,

$$t = \frac{r_A + r_O}{\sqrt{2}(r_B + r_O)} \quad (2)$$

where, r_A , r_B and r_O are the effective radii of the A-site cation, B-site cation and the oxygen ion respectively. Tolerance factor is a quantitative measure of the mismatch between the bonding requirements of the A-site and B-site cations in the perovskite ABO_3 and subsequently reflects the structural distortion such as rotation and tilt of the octahedral. Since the substituent at A-site ionic radii are lesser compare to Pb so tilt as well as non-centrosymmetric distortion will reduce. It is also reflected with the merging of peaks in XRD that indicate from non-centrosymmetric to centrosymmetric structure. Again we need to mention that for tolerance factor ~ 1 , a perovskite phase is expected [16-17]. The tolerance factor of the PNST- x samples decreases from 1.019 as in $x=0$ to 0.988 for $x=0.5$ [table 1]. Hence, the general tendency of these structures is to be in the perovskite phase as $t \sim 1$. Also notice the strong similarity between the nature of decrement of the c -axis with the reduction in effective ionic radius of the A-site although a -axis is invariant. This indicates that Na/Sm substitution does not influence the a -axis but varies proportionately the c -axis. Microstructure studies were performed of PNST- x compounds. The average grain size with standard deviation decreases from $1.03 \pm 0.36 \mu\text{m}$ as in $x=0.10$ to $0.60 \pm 0.17 \mu\text{m}$ for $x=0.50$ with substitution are reported in table. 1. Microstructure of fracture surface of $x=0.40$ was shown in Fig. 1a.

There is a subtle balance between the long-range Coulomb interaction and short-range forces in materials. Domain structure and defect determine the long range Coulomb interaction which in turn makes the ferroelectric transitions highly sensitive. Such changes lead to the splitting of longitudinal optical (LO) and transverse optical (TO) phonons [18-19]. Hence Raman spectroscopy is an excellent tool in qualitatively assessing retention of domain structure, defects and structural distortions thereby understand deformations and lattice strains associated with substitution in ferroelectrics like in PNST- x .

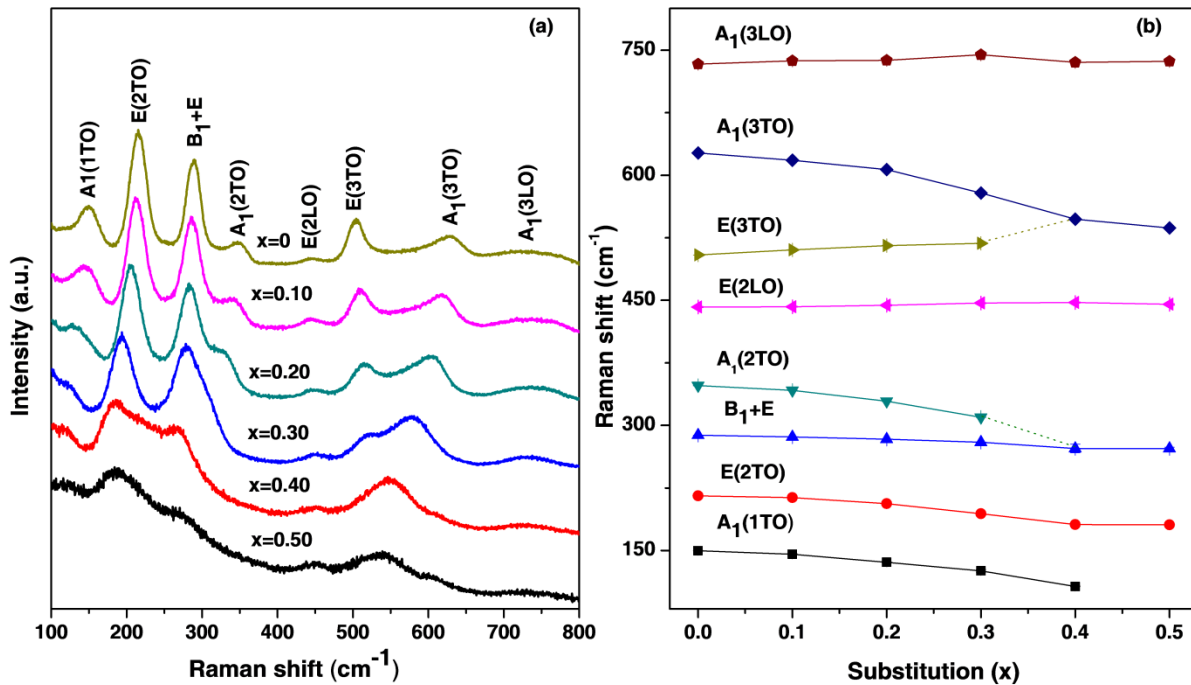


Fig. 2. (a) HR Raman spectroscopic measurement of the compounds $\text{Pb}_{(1-x)}(\text{Na}_{0.5}\text{Sm}_{0.5})_x\text{TiO}_3$ $0 \leq x \leq 0.5$. (b) Variations of mode after fitting the Raman data.

The Raman spectra of PNST- x are shown in Fig. 2a. All the phonon vibrations of these compounds correspond to known vibrational modes of pure PbTiO_3 . Intensities decreased, peak widths increased and positions varied for different modes with substitution. The cubic paraelectric phase of pure PbTiO_3 belongs to the space group with 12 optic modes at the point of the Brillouin zone in the $3T_{1u}+T_{2u}$ representation of the O_h point group. The $3T_{1u}$ modes are Raman inactive but infrared active while T_{2u} modes (silent modes) are both Raman and infrared inactive. Therefore the cubic phase has no Raman active modes [20-22]. Although in XRD we see that the lattice is becoming cubic, the very fact that in our samples Raman modes is visible up to $x=0.50$, hints at retention of ferroelectricity until $x=0.50$. After fitting the Raman data, energy variations of the phonon modes with composition are observed [Fig. 2b]. Except $A_1(3\text{LO})$, $E(3\text{TO})$ and $E(2\text{TO})$ which are blue shifted, all other modes are red shifted.

The $A_1(1\text{TO})$ transverse optical mode relates to the relatively opposite vibrations of the $O\text{-B-O}$ chains to the Pb sub lattice along c -axis in the ABO_3 perovskite structure. It is also dependent on the displacement of the BO_6 octahedron relative to Pb atoms [23-24]. It has a direct relation to the order parameter. $A_1(1\text{TO})$ is generally called “soft mode” due to losing energy as the sample undergoes a tetragonal to cubic phase transition [25-26]. In PNST- x , $A_1(1\text{TO})$ mode loses intensity and energy with increasing substitution indicating a direct relation to our XRD results. Reduction in the energy is a direct consequence of the reduction in the c -axis in spite of reduction of effective mass of the A-site. Such a reduction may be due to increase of lattice distortions due to Na/Sm introduction. Please note that the energy of $A_1(3\text{TO})$ reduces while $E(3\text{TO})$ modes marginally increases to merge in $x=0.4$ sample. The relative vibrational motion of the Ti atoms with respect to the oxygen atoms along the $O\text{-Ti-O}$ chains along c -axis result in $A_1(3\text{TO})$ soft modes. As TO modes vibrate along the direction of the spontaneous polarization (c -axis) in PbTiO_3 , the $A_1(3\text{TO})$ mode is very important. The $E(3\text{TO})$ mode is one of the modes which has gained energy. This mode is a result of vibrations of Ti and planar O ions with respect to each other along the ‘ a ’ and ‘ b ’ axes. Please note, in parent PbTiO_3 , the displaced off-centered Ti ion is at a strained bonding with the planar oxygen. With the reduction in tetragonality, these Ti ions will be nearer to the O -plane and the structure will become more centro-symmetric. Thereby the strain in the $O\text{-Ti-O}$ bond will be reduced and the ions will be capable of vibrating more energetically. In congruence with our XRD results the reduction of tetragonality is also reflected in our Raman results.

Dielectric measurement is a powerful tool to study the effect of Na/Sm substitution on the phase transition of the PNST- x ceramics. A phase pure, sufficiently dense and mechanically robust PbTiO_3 pellet was extremely difficult to fabricate and hence dielectric property of PbTiO_3 phase was not investigated. With substitution preparation of pellets, appropriate for dielectric measurements, became easier and dielectric properties including dielectric constant, impedance, capacitance and dielectric loss factor were measured in the temperature range 300-750 K for

various frequencies in 10 Hz – 1 MHz range. Here we will concentrate on the dielectric constant only to discuss a probable ferroelectric to paraelectric phase transition of these materials.

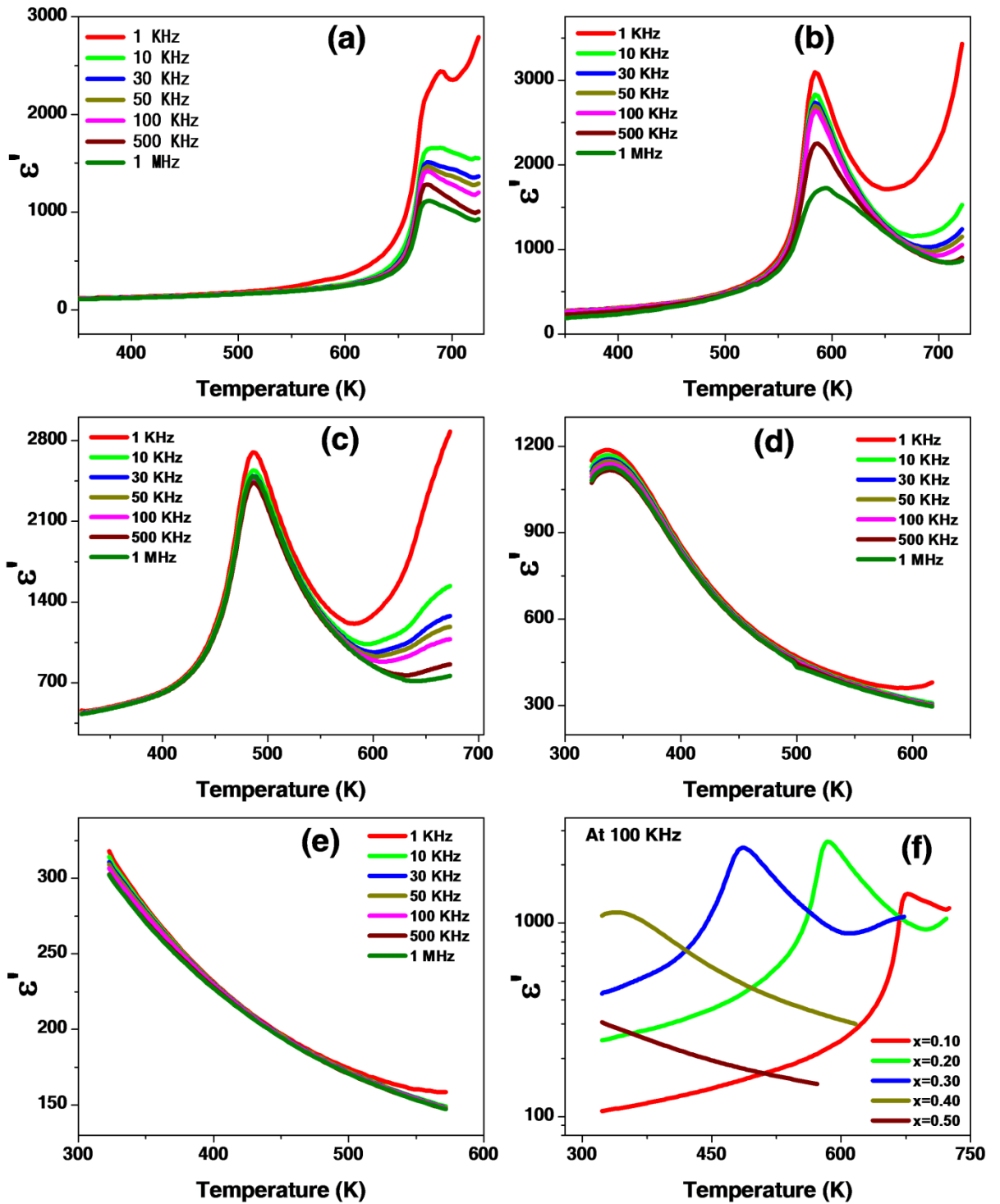


Fig. 3. Temperature dependent dielectric constant of $\text{Pb}_{(1-x)}(\text{Na}_{0.5}\text{Sm}_{0.5})_x\text{TiO}_3$ for composition (a) $x=0.10$, (b) $x=0.20$, (c) $x=0.30$, (d) $x=0.40$, (e) $x=0.50$, (f) Dielectric constant vs temperature at 100 kHz for $0.10 \leq x \leq 0.50$ composition.

Temperature dependent dielectric constant [Fig. 3(a-e)] for different fixed frequencies as a function of temperature for PNST- x ceramics shows peaks above room temperature for all samples except for $x=0.5$. The temperature of dielectric maximum, T_m , decreases with increasing substitution from ~ 677 K in $x=0.1$ to ~ 338 K in $x=0.4$ for all frequencies. At 1 kHz, ϵ' - T peak around 670 K seems to be overshadowed by some other phenomenon. This may be a space-charge polarization effect. Values of dielectric constant at T_m for $x=0.1$ show significant frequency dispersion. The $x=0.5$ sample shows a gradually decreasing ϵ' with increase in temperature in the entire range suggesting T_m below room temperature. It can be further noticed that the frequency dispersion in dielectric constant around T_m decreases with increasing Na/Sm content. Such frequency dispersion trend can be explained by the incidence of space charge polarization which becomes significant at low frequencies and high temperatures [27].

Pure PbTiO_3 is known to have a sharp ferroelectric to paraelectric transition around 763 K (Curie temperature) accompanied by a structural transition from polar tetragonal to non-polar cubic phase [28]. This structural phase transition manifests as a sharp and frequency independent peak in dielectric permittivity versus temperature plot. Fig. 3f shows ϵ' as a function of temperature measured at 100 kHz for various PNST- x samples. It can be clearly seen that the temperature of dielectric maximum decreases linearly with increasing x . $\text{Pb } 6s^2$ lone pair electrons help in stabilizing the large tetragonal strain ($\sim 6\%$) in PbTiO_3 . Our XRD analysis confirmed that $\text{Na}^+/\text{Sm}^{3+}$ substitution at Pb^{2+} (with $6s^2$ lone pair) site modifies the tetragonal strain in PbTiO_3 and finally for $x=0.5$ exhibits a ‘cubic’ structure. Note that such a structural change is also reflected in phase transition temperature, Na/Sm substitution requiring lesser thermal energy for the ferroelectric-paraelectric phase transition. Similar trend has been observed in other perovskite related ferroelectrics [15, 29].

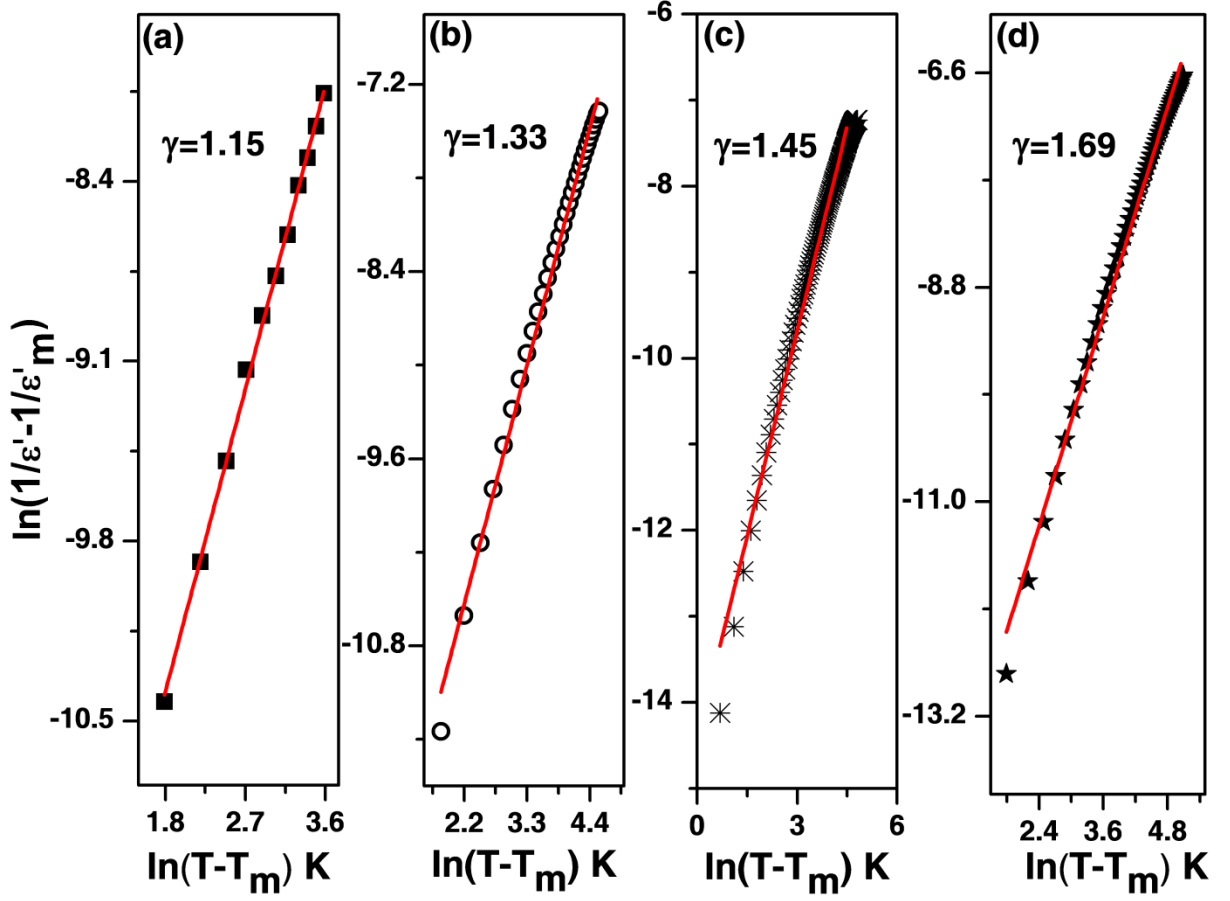


Fig. 4. Plot between $\ln\left(\frac{1}{\varepsilon'} - \frac{1}{\varepsilon'_m}\right)$ versus $\ln(T - T_m)$ with linear fitting of the compound PNST- x at 100 kHz. Where solid lines are representing the fitted data and symbols experimental data.

Diffuse phase transition is usually observed in perovskites with random distribution of different types of ions on structurally identical sites in lattice [30-31]. It must be noted that diffuse phase transition exhibit a broad instead of a sharp change of structure and properties at the Curie point in normal ferroelectric materials [32-33]; consequently, the phase transition characteristics of such materials are known to diverge from the characteristic Curie-Weiss behavior and can be described by a modified Curie-Weiss formula [34].

$$\frac{1}{\varepsilon'} - \frac{1}{\varepsilon'_m} = C^{-1}(T - T_m)^\gamma \quad (3)$$

where, C is Curie-Weiss constant and the degree of diffuseness, γ ($1 \leq \gamma \leq 2$; where $\gamma=1$ gives a sharp change while an ideal diffuse phase transition gives $\gamma=2$). An apparent increase in diffuseness of peak in $\varepsilon'-T$ plots is reflected in the least-square linear fitting of $\ln\left(\frac{1}{\varepsilon'} - \frac{1}{\varepsilon'_m}\right)$ versus $\ln(T - T_m)$ curves [Fig. 4] at a frequency of 100 kHz of PNST- x ceramics. A reasonably good fit is observed for all compositions. The degree of diffuseness, γ was calculated from the

slop of linear fit. γ was found to increases from 1.15 ± 0.02 for $x=0.1$ to 1.69 ± 0.01 for $x=0.5$ indicating a significant increase in diffuseness of phase transition in doped samples. Compositional disorder arising due to the random distribution of Na^+/Sm^{3+} seems to be responsible for observed diffuse phase transition in PNST- x ceramics [33]

Table. 1. Room temperature dielectric constant and loss, average grain size, tolerance factor, phase transition temperature, apparent remnant polarization and coercive field for the compounds PNST- x .

Substitution (x)	ϵ' (100 kHz)	Tan δ (100 kHz)	Average grain size ($\sim \mu\text{m}$)	Tolerance factor (t)	T_m (K)	$2P_r$ ($\mu\text{C}/\text{cm}^2$)	$2E_C$ (kV/cm)
0.10	178	0.012	1.03 ± 0.36	1.019	677	0.43	14.82
0.20	236	0.017	0.88 ± 0.25	1.013	584	2.14	25.84
0.30	397	0.026	0.67 ± 0.24	1.007	486	47.65	43.25
0.40	1225	0.038	0.60 ± 0.25	1.001	338	18.56	16.99
0.50	364	0.073	0.60 ± 0.17	0.995

(Fig. S1) Room temperature dielectric constant (ϵ') of PNST- x ceramics gradually increases with increasing x in the range $0.10 \leq x \leq 0.40$ and thereafter decreases for $x=0.5$ (Table. 1). This behavior can be attributed to the higher polarizability of Na and Sm than Pb [35]. The decrease in ϵ' in $x=0.5$ is due to the paraelectric phase of the sample at room temperature whereas the other samples are in ferroelectric phase.

To confirm the ferroelectricity in PNST- x , polarization versus electric field (P - E) hysteresis loop measurements were carried out for all the compositions. The hysteresis loops were measured at a frequency of 1 Hz at room temperature. For composition with $x=0.10$, [Fig. 5], P - E hysteresis loops are not typical ferroelectric loops but are more like those usually obtained for lossy dielectric materials [36]. Observed apparent remnant polarization and coercive field values at an applied electric field $\sim 50 \text{ kV}/\text{cm}$ for all the samples are given in Table1. P - E hysteresis loops obtained for compositions with $x = 0.20, 0.30,$ and 0.40 are typical hysteresis loops obtained for ferroelectric ceramics while an almost linear relation between P and E is observed for composition with $x=0.50$. This suggests that sample with $x=0.50$ is macroscopically in paraelectric state at room temperature and it is expected as corroborated by the XRD, Raman and dielectric studies. Sample with composition $x=0.30$ shows the highest apparent remanent polarization of $47.65 \mu\text{C}/\text{cm}^2$ and a coercive field of $43.25 \text{ kV}/\text{cm}$ at an applied electric field of $50 \text{ kV}/\text{cm}$.

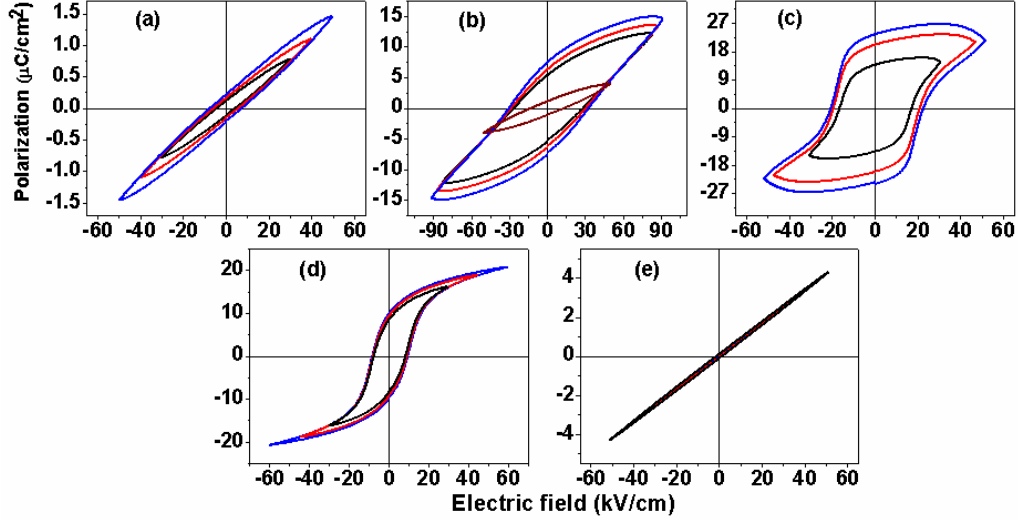
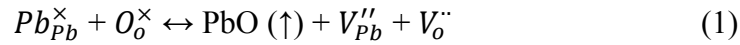


Fig. 5. P - E loop measurement of the samples PNST- x , (a) $x=0.10$, (b) $x=0.20$, (c) $x=0.30$, (d) $x=0.40$, and (e) $x=0.50$

From the structural point of view, composition with $x=0.10$ is expected to be ferroelectric. However, at applied electric fields up to 50-60 kV/cm , no signature of domain switching (or ferroelectric ordering) is discernable in P - E hysteresis loops. It was not possible to apply more voltage due to high leakage current in this composition [37].

Drastic improvement in room temperature ferroelectric properties in Na/Sm doped samples can be attributed to the cumulative effect of improved density, reduced volatilization of Pb , associated oxygen vacancies, increased dielectric constant and reduced tetragonal strain. It is well known that oxygen vacancies are created due to Pb loss during high-temperature sintering of $PbTiO_3$ based perovskite ceramics and are expressed by following Kröger-Wink equation:



These oxygen vacancies can hop easily due to their high mobility in applied high electric field and accumulate in the places with low free energy, such as domain walls and grain boundaries. Accumulation of these oxygen vacancies at the domain boundary causes domain pinning which restricts polarization switching [38-39].

Conclusion

Sodium (Na) and samarium (Sm) doped $PbTiO_3$ ceramic samples PNST- x have been successfully synthesized by the modified Pechini sol-gel process. Phase confirmation was shown by X-ray diffraction pattern of the $Pb_{(1-x)}(Na_{0.5}Sm_{0.5})_xTiO_3$ ($0 \leq x \leq 0.5$) samples. From HR Raman spectroscopy measurement, we investigated the variations of vibrational modes with composition and also relate with ferroelectric property. High temperature dielectric study was done to see the variations of the phase transition temperature with composition. Decrease of phase transition temperature is due to replacement of Pb ($6s^2$) by less average ionic radii of Na/Sm . Diffuse type phase transition behavior was calculated by modified Curie-Weiss law and it was concluded due to random distribution of Na/Sm at the Pb site. These dielectric materials are important for technical applications.

Acknowledgement

One of the authors Arun Kumar Yadav is grateful to the university Grants Commission to award me fellowship (NFO-2015-17-OBC-UTT-28455). Principle investigator expresses sincere thanks to Indian Institute of Technology, Indore for funding the research and also using the Sophisticated Instrument Centre (SIC) for the research.

References

1. Paris EC, Gurgel MFC, Joya MR, Casali GP, Paiva-Santos CO, Boschi TM, Pizani PS, Varela JA, Longo E (2010) Structural deformation monitored by vibrational properties and orbital modeling in (Pb,Sm)TiO₃ systems. *J. Phys. Chem. Solids* 71:12–17
2. Hlinka J, Kempa M, Kulda J, Bourges P, Kania A, Petzelt J (2006) Lattice dynamics of ferroelectric PbTiO₃ by inelastic neutron scattering. *Phys. Rev. B* 73:140101
3. Tomeno I, Fernandez-Baca JA, Marty KJ, Oka K, Tsunoda Y (2012) Simultaneous softening of acoustic and optical modes in cubic PbTiO₃. *Phys. Rev. B* 86:134306
4. Shigematsu H, Nakadaira H, Futatsugi T, Matsui T (2000) Ti-isotope effect on ferroelectric phase transition of PbTiO₃ studied by heat capacity measurement. *Thermochim Acta* 352-353:43-46
5. Jaouen N, Dhaussy AC, Itié JP, Rogalev A, Marinel S, Joly Y (2007) High-pressure dependent ferroelectric phase transition in lead titanate. *Phys. Rev. B* 75:224115
6. Zhang Q, Zhu X, Xu Y, Gao H, Xiao Y, Liang D, Zhu J, Zhu J, Xiao D (2013) Effect of La³⁺ substitution on the phase transitions, microstructure and electrical properties of Bi_{1-x}La_xFeO₃ ceramics. *J. Alloys Comp.* 546:57-62
7. Szabó GS, Cohen RE, Krakauer H (1998) First-Principles Study of Piezoelectricity in PbTiO₃. *Phys. Rev. Lett.* 80:4321
8. Chen J, Shi H, Liu G, Cheng J, Dong S (2012) Temperature dependence of dielectric, piezoelectric and elastic properties of BiScO₃–PbTiO₃ high temperature ceramics with morphotropic phase boundary (MPB) composition. *J. Alloys Comp.* 537:280-285
9. Shah DD, Mehta PK, Desai MS, Panchal CJ (2011) Origin of giant dielectric constant in Ba[(Fe_{1-x}Co_x)_{1/2}Nb_{1/2}]O₃. *J. Alloys Comp.* 509:1800-1808
10. Forrester JS, Zobec JS, Phelan D, Kisi EH (2004) Synthesis of PbTiO₃ ceramics using mechanical alloying and solid state sintering. *J. Solid State Chem.* 177:3553-3559
11. Alguero M, Ramos P, Jimenez R, Amorin H, Vila E, Castro A (2012) High temperature piezoelectric BiScO₃–PbTiO₃ synthesized by mechanochemical methods. *Acta Mater.* 60:1174-1183
12. Wu Z, Cohen RE (2005) Pressure-Induced Anomalous Phase Transitions and Colossal Enhancement of Piezoelectricity in PbTiO₃. *Phys. Rev. Lett.* 95:037601
13. Bokov AA (1992) Recent advances in diffuse ferroelectric phase transitions. *Ferroelectrics* 131:49-55
14. Bokov AA, Shpak LA, Rayevsky IP (1993) Diffuse phase transition in Pb(Fe_{0.5}Nb_{0.5})O₃-based solid solutions. *J. Phys. Chem. Solids* 54:495-498

15. Abdelmoula N, Chaabane H, Khemakhem H, Vonder Mühl R, Simon A (2006) Relaxor or classical ferroelectric behavior in A-site substituted perovskite type $Ba_{1-x}(Sm_{0.5}Na_{0.5})_xTiO_3$. *Solid State Sci.* 8:880-887
16. Woodward DI, Reaney IM (2005) Electron diffraction of tilted perovskites. *Acta Crystallogr., Sect. B: Struct. Sci* B61: 387-399
17. Zhao W, Zuo R, Li F, Li L (2014) Structural, dielectric, ferroelectric and strain properties in $CaZrO_3$ -modified $Bi(Mg_{0.5}Ti_{0.5})O_3$ - $PbTiO_3$ solid solutions. *J. Alloys Comp.* 591:218-223
18. Zhong W, King-Smith RD, Vanderbilt D (1994) Giant LO-TO Splitting in Perovskite ferroelectrics. *Phys. Rev. Lett.* 72:3618-3621
19. Mani BK, Chang CM, Ponomareva I (2013) Atomistic study of soft-mode dynamics in $PbTiO_3$. *Phys. Rev. B* 88:064306
20. Burns G, Scott BA (1973) Lattice Modes in Ferroelectric Perovskites: $PbTiO_3$. *Phys. Rev. B* 7:3088
21. Foster CM, Li Z, Grimsditch M, Chan SK, Lam DJ (1993) Anharmonicity of the lowest-frequency $A_1(TO)$ phonon in $PbTiO_3$. *Phys. Rev. B* 48:10160
22. Sanjurjo JA, Cruz EL, Burns G (1983) High-pressure Raman study of zone-center phonons in $PbTiO_3$. *Phys. Rev. B* 28:7260
23. Sun C, Wang J, Hu P, Kim MJ, Xing X (2010) Effects of Al substitution on the spontaneous polarization and lattice dynamics of the $PbTi_{1-x}Al_xO_3$. *Dalton Trans.* 39:5183.
24. Paris EC, Gurgel MFC, Boschi TM, Joya MR, Pizani PS, Souza AG, Leite ER, Varela JA, Longo E (2008) Investigation on the structural properties in Er-doped $PbTiO_3$ compounds: A correlation between experimental and theoretical results. *J. Alloys Comp.* 462:157-163
25. Sun L, Chen YF, He L, Ge CZ, Ding DS, Yu T, Zhang MS, Ming NB (1997) Phonon-mode hardening in epitaxial $PbTiO_3$ ferroelectric thin films. *Phys. Rev. B* 55:12218
26. Cho SM, jang HM (2000) Softening and mode crossing of the lowest-frequency A_1 (transverse-optical) phonon in single-crystal $PbTiO_3$. *Appl. Phys. Lett.* 76:3014-3016
27. Wu D, Li A, Ming N (2004) Dielectric characterization of $Bi_{3.25}La_{0.75}Ti_3O_{12}$ thin films. *Appl. Phys. Lett.* 84:4505-4507
28. Gu H, Hu Y, You J, Hu Z, Yuan Y, Zhang T (2007) Characterization of single-crystalline $PbTiO_3$ nanowire growth via surfactant-free hydrothermal method. *J. Appl. Phys.* 101: 024319
29. Bhaskar S, Majumder SB, Katiyara RS (2002) Diffuse phase transition and relaxor behavior in $(PbLa)TiO_3$ thin films. *Appl. Phys. Lett.* 80:3997
30. Singh A, Chatterjee R (2012) Multiferroic Properties of La-Rich $BiFeO_3$ - $PbTiO_3$ Solid Solutions. *Ferroelectrics* 433:180
31. Jiang XP, Fang JW, Zeng HR, Chu BJ, Li GR, Chen DR, Yin QR (2000) The influence of $PbZrO_3/PbTiO_3$ ratio on diffuse phase transition of $Pb(Zn_{1/3}Nb_{2/3})O_3$ - $PbZrO_3$ - $PbTiO_3$ system near the morphotropic phase boundary. *Mater. Lett.* 44:219-222

32. Nakamura T, Takashige M (1990) Diffuse phase transition and low temperature dielectric constant in PbTiO_3 . *Ferroelectrics* 108:159-164
33. Chen J, Qi Y, Shi G, Yan X, Yu S, Cheng J (2008) Diffused phase transition and multiferroic properties of $0.57(\text{Bi}_{1-x}\text{La}_x)\text{FeO}_3-0.43\text{PbTiO}_3$ crystalline solutions. *J. Appl. Phys.* 104:064124
34. Ji W, He X, Cheng W, Qiu P, Zeng X, Xia B, Wang D (2015) Effect of La content on dielectric, ferroelectric and electro-optic properties of $\text{Pb}(\text{Mg}_{1/3}\text{Nb}_{2/3})\text{O}_3-\text{PbTiO}_3$ transparent ceramics. *Ceram. Int.* 41:1950-1956
35. <http://ctcp.massey.ac.nz/Tablepol2014.pdf>
36. Scott JF (2008) Ferroelectrics go bananas. *J. Phys.: Condens. Matter* 20:021001.
37. AJ Priyanka, KJ Pardeep, Jha A. K., Kotnala RK, Drivedi RK (2014) Phase transformation and two-mode phonon behavior of $(1-x)[\text{Ba Zr}_{0.025}\text{Ti}_{0.975}\text{O}_3]-(x) [\text{BiFeO}_3]$ solid solutions. *J. Alloys Comp.* 600:182-196.
38. N Yuji, M Ichiro, G Yu, M Masaru (2000) Defect control for large remanent polarization in bismuth titanate ferroelectrics—doping effect of higher-valent cations. *Jpn. J. Appl. Phys.* 39:L1259-L1262.
39. K Sunil, Verma K.B.R. (2009) Influence of lanthanum doping on the dielectric, ferroelectric and relaxor behaviour of barium bismuth titanate ceramics. *J. Phys. D: Appl. Phys.* 42:075405.